ADVANCED FUNCTIONAL MATERIALS



# Pattern-Transfer Fidelity in Soft Lithography: The Role of Pattern Density and Aspect Ratio**

By *Tae-Woo Lee*,* *Oleg Mitrofanov*, and *Julia W. P. Hsu*

Using high-aspect-ratio nanostructures fabricated via two-photon laser-scanning lithography, we examine the deformation of elastomeric stamps used in soft nanolithography and the fidelity of patterns and replicas made using these stamps. Two-photon laser-scanning lithography enables us to systematically regulate the aspect ratio and pattern density of the nanostructures by varying laser-scanning parameters such as the intensity of the laser beam, the scanning speed, the focal depth inside the resist, and the scanning-line spacing. Two commercially available stamp/mold materials with different moduli have been investigated. We find that the pattern-transfer fidelity is strongly affected by the pattern density. In addition, we demonstrate that true three-dimensional structures can be successfully replicated because of the flexible nature of elastomeric poly(dimethylsiloxane).

## 1. Introduction

Over the past decade, soft lithography[1] has become an important tool in nanofabrication with a wide variety of applications[2] from biology to engineering. The common thread in soft-lithography techniques is the use of conformable, elastomeric stamps or molds that are prepared by curing rubber-like siloxane materials such as poly(dimethylsiloxane) (PDMS) on microstructured or nanostructured "masters". The masters are typically photoresist patterns generated by conventional optical or electron-beam lithography, but not limited to these methods. Since a master can be used to make many stamps/molds and each stamp/mold can be used several times, soft-lithography approaches reduce costs and are scalable for manufacturing purposes. The two most widely used soft-lithography techniques are microcontact printing and replica molding.[1,2] In microcontact printing, a patterned self-assembled monolayer (SAM) is transferred or stamped onto the surface; this patterned SAM can then be used as an etch mask to produce metallic nanostructures[1,2] or as a template to direct inorganic-crystal growth.[3] Replica molding uses elastomeric molds and UV- or thermally curable epoxy to make inexpensive replications of the masters; it has been explored for making polymeric photonic devices.[4,5] For all applications, the fidelity of pattern transfer is the most important issue. Therefore, this work is focused on how much a transferred (i.e., printed or replicated) pattern resembles the master, how many defects in the transferred pattern are generated during the process, and what causes defect formation. Many factors influence the pattern-transfer fidelity, including feature size, aspect ratio, pattern density, sidewall profile, stamp/mold material, and processing conditions. In particular, the pattern density becomes more important as the feature size is pushed down to the nanoscale. This effect has not been studied in previous soft-lithography works.[6,7] In this work, we systematically investigate the influence of aspect ratio and pattern density on pattern-transfer fidelity in microcontact printing and replica molding using nanostructures generated by two-photon lithography as masters. We tested two commercially available PDMS materials for the stamps/molds in order to investigate the effect of stamp/mold modulus. We found that, along with aspect ratio, pattern density plays an important role.

High-aspect-ratio nanostructures are desired in many soft-lithography applications. However, they are difficult to make using conventional photolithography based on a one-photon-absorption process. Photopolymerization based on two-photon absorption provides a solution to generate high-aspect-ratio and complex three-dimensional (3D) polymeric features with subdiffraction-limited spatial resolution.[8–13] Because the two-photon absorption occurs only in the vicinity of the focal point due to the quadratic dependence on the excitation intensity, and the polymerization process occurs only if the intensity reaches a polymerization threshold,[14–16] arbitrarily shaped 3D structures can be generated with high resolution via two-photon-initiated photopolymerization of polymer resins. Thus, it is possible to vary the aspect ratio (height/width) and spacing of patterns using this method. To test the pattern-transfer fidelity, we created masters containing nanostructures with different aspect ratios and pattern densities by systematically varying laser-scanning parameters, including the intensity of the laser beam, the scanning speed, the focal depth inside the resist, and the scan-line spacing.

Another important factor in soft lithography is the mechanical properties of the stamps/molds. Most work on molding and contact printing has been done using Sylgard 184 (Midland, MI), a commercially available thermocurable siloxane polymer. However, the low compression modulus (2.0 $N\,mm^{-2}$) of Sylgard 184 PDMS causes the stamp to deform, buckle, or col-

[*] Dr. T.-W. Lee, Dr. O. Mitrofanov, Dr. J. W. P. Hsu
Bell Laboratories, Lucent Technologies
600 Mountain Avenue, Murray Hill, NJ 07974 (USA)
E-mail: taew.lee@samsung.com

[**] We acknowledge Dr. J. A. Rogers for his technical help and comments, and Dr. H. Cho for helpful comments. This work was partially supported by the Korea Science & Engineering Foundation.

 DOI: 10.1002/adfm.200400295  

lapse.[6] For the high-aspect-ratio structures, the most relevant deformation mode of PDMS stamps/molds is lateral collapse.[6] Patterns with features smaller than 1 μm in size require more rigid mechanical properties of the stamp. Schmid and Michel formulated a polymeric composite based on vinyl and hydrosilane end-linked polymers, called "hard PDMS" (h-PDMS), which has a higher compression modulus ($\approx 9\ \mathrm{N\,mm^{-2}}$).[7] They demonstrated replication of high-density patterns at the 100 nm scale.[7] In this work, we compared the performance of these two commercially available PDMS materials (Sylgard 184 vs. h-PDMS) for soft-lithography applications.

## 2. Results and Discussion

High-aspect-ratio nanostructures were fabricated in commercial negative-photoresist films (SU8-5, Micro Chem Corp.) by scanning a focused laser beam to induce photopolymerization in selected regions. Two-photon absorption induced polymerization occurs only in the high-intensity region of the tightly focused laser beam because the two-photon absorption process is proportional to the intensity squared.[14,15] Linear absorption at the laser wavelength (710 nm) does not cause the polymerization process; therefore the focal point can be placed below the surface, resulting in local polymerization inside the film. The two-dimensional nanostructures used in this experiment were made by scanning the focused laser spot first along one direction, and then along another direction either at 45° (Fig. 1b) or 90° (Fig. 1c) to the first, using the setup depicted in Figure 1a. The resulting structures had enough mechanical stability so that the high-aspect-ratio structures did not bend or distort during the developing process. Typical patterns of area $\approx 100\ \mu\mathrm{m} \times 100\ \mu\mathrm{m}$ were made in a few minutes. The parameters that determine spatial resolution and aspect ratio in the two-photon nanolithography are the numerical aperture, the laser power, and the exposure time. We controlled the exposure time by varying the scan speed. A laser beam above a certain threshold power for a certain exposure time was needed to induce polymerized structures. We obtained aspect ratios as high as seven.

We can further modify the perfectly periodic structures by exposing the latent SU8 image to additional laser exposure at specifically chosen positions. Figures 2a,d show examples of modified periodic patterns fabricated by two-photon polymerization. Figure 2a shows that a single column of holes, with a length exceeding 35 μm, has been filled in. In Figure 2d, the precision control of our two-photon setup is demonstrated by writing a "Y-shaped" figure. Its bottom "trunk" was made by precisely filling in 14 holes in a single column, and the two "arms" (of diagonal length equal to 9 holes) are at 45° to the trunk. This demonstrates the potential of using two-photon lithography for making non-periodic structures, for example, waveguides and microresonators in photonic-bandgap structures.[11–13,15]

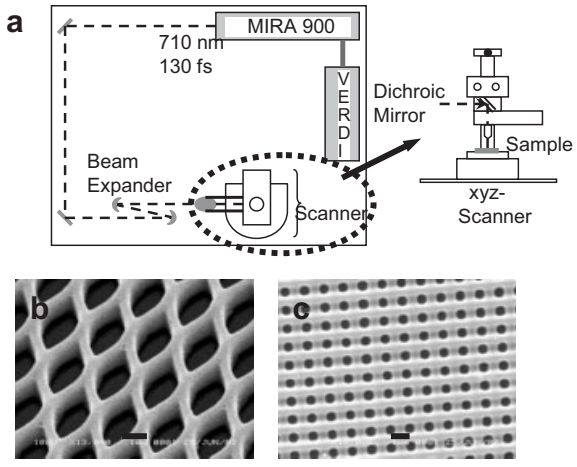


**Figure 1.** a) Schematic illustration of laser-scanning microscope setup used for two-photon lithography. The light source in our two-photon laser-scanning microscope is a femtosecond Ti:sapphire laser (Coherent Mira900) with a short wavelength mirror set, pumped by a 5 W, frequency-doubled Nd:$YVO_4$ laser (Coherent Verdi). The pulse length of 130 fs was maintained at 710 nm. The laser beam was then expanded and collimated using spherical mirrors before it entered the laser-scanning microscope. The dichroic beamsplitter at the laser input port has a high transmission, between 320 and 650 nm, and good reflectivity, between 700 and 850 nm. The samples were loaded on top of an *xyz* scanner. b) Scanning electron microscopy (SEM) image of an SU8 nanostructure 1.67 μm tall with an aspect ratio of 5.6 (297 nm line width), which has diamond holes in a honeycomb lattice; the second scan was at 45° to the first. The scan rate was $66\ \mu\mathrm{m\,s^{-1}}$, and the laser power was 5 mW. c) SEM image of an SU8 nanostructure 1.51 μm tall with an aspect ratio of 3.8 (401 nm linewidth), which has rectangular holes in a square lattice; the second scan was at 90° to the first. The scan rate was $44\ \mu\mathrm{m\,s^{-1}}$, and the laser power was 5 mW. The scale bars are 1 μm.

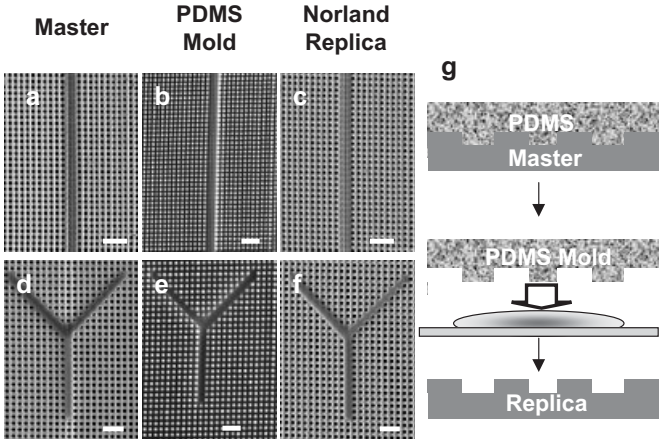


**Figure 2.** SEM images showing the replication of a line (a) and a Y-shaped "defect" (d) in otherwise perfectly periodic nanostructures fabricated by two-photon lithography. PDMS was cast and cured on the master pattern to give molds (b,e). Then the PDMS molds were cut and cured on Norland optical adhesive (NOA) to give the final replica molds (c,f). The molding process is illustrated in (g). All images were taken using a scanning electron microscope. The scale bars are 5 μm.

  

ADVANCED FUNCTIONAL MATERIALS



Figure 2g illustrates the replication process used in soft lithography. Figures 2b,e are the PDMS molds (Sylgard 184) made from the masters shown in Figures 2a,d, respectively. The holes in the masters become posts in the molds. Note that lateral collapse between adjacent posts did not occur for these structures. Finally, epoxy replicas (NOA73) are shown in Figures 2c,f. It is clear that the submicrometer-sized features in the masters have been faithfully reproduced across a large area.

To investigate possible deformation of the PDMS molds, we used two-photon lithography to fabricate nanostructures with different aspect ratios and pattern densities. Since the two-photon beam can be focused deep inside the film, we regulated the pattern height by regulating the focal depth. The aspect ratios of the patterns were controlled by the intensity and scanning rate (i.e., exposure dose) of the laser beam. The master with periodic holes can be molded with PDMS to give periodic posts. With these PDMS molds, we microcontact printed thin (≈15 nm) gold films to make patterned gold nanostructures and made epoxy replicas in order to examine the pattern-transfer fidelity. We compared two different commercially available PDMS materials (h-PDMS and Sylgard 184). We first inspected the as-made PDMS stamps/molds. We inspected them again after inking them in a SAM solution during microcontact printing and after the entire soft-lithography process. We also inspected the etched gold patterns and the epoxy replicas.

Figure 3 shows gold patterns made by microcontact printing and chemical etching using PDMS stamps with two different pattern densities and several different aspect ratios. Pattern density is defined as the ratio of post area ($\pi r^2$, where $2r$ is the diameter of the post) divided by the unit cell area ($l^2$, where $l$ is the distance between the centers of two nearest-neighbor posts), i.e., $\pi r^2/l^2$. In general, the patterns made using composite h-PDMS stamps contain fewer defects compared with those made with Sylgard 184. As the aspect ratio increases, the patterns show increasing lateral collapsed defects, i.e., the two neighboring posts of the PDMS stamps tend to merge. When we compared patterns with the same aspect ratio but different pattern densities (Figs. 3b,c), the pattern with the higher density tended to have more defects. After observing these phenomena, we tried to clarify whether this collapsing happened during inking of the hexadecanethiol (HDT) ethanol solution or during printing of the ink on the gold surface using the PDMS stamps. We found that most of the collapsing happened during the inking process. This was caused by the surface tension of the ethanol (22.1 mN m$^{-1}$ at 20 °C), which makes the PDMS posts bend and merge together when the post spacing is small.

It has been experimentally demonstrated that, at large aspect ratios, the pillars can collapse under their own weights (buckling), or they can adhere to each other laterally (lateral collapse) when capillary and other forces acting on them are sufficiently large to cause contact between them.[7] In the microcontact-printing process, the PDMS stamps can deform because of 1) surface tension due to inking and solvent evaporation, and 2) contact-associated deformation under pressure. Since we observed stamp deformation after inking, the first process is the

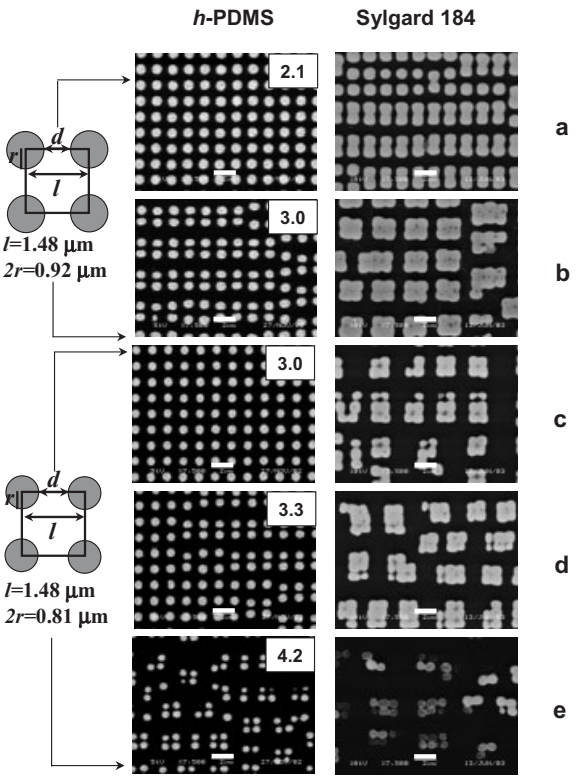


**Figure 3.** SEM images of microcontact printed and etched gold patterns on silicon wafers with changing aspect ratio and pattern density, using two different PDMS stamps (h-PDMS and Sylgard 184). A 2 mM ethanolic solution of hexadecanethiol was used as the ink in the microcontact printing. The numbers in the top right corners in the left images indicate the aspect ratios of the posts of the stamps. The images are classified into two different pattern densities: 0.303 (a,b) and 0.235 (c–e). All scale bars are 2 μm.

dominant cause of the low pattern-transfer fidelity shown in Figure 3. The distances of the gaps between the patterns and their aspect ratios are the critical factors in determining whether deformation or collapse occurs.[17] In addition, the surface tension between the pillars during the drying of the HDT ethanol solution and the moduli of the patterning materials affect the deformation. The critical Young's modulus of the pattern ($E_c$) at stable/distorted boundaries is given by Equation 1[18]

$$E_c = 24\sigma H^4/(2r)^3 d^2 \quad (1)$$

where $\sigma$ is the surface tension, $d$ is the gap distance between the pillars, and $H$ is the pattern height. As $E_c$ is inversely proportional to the quadratic power of the gap distance, $d^2$, and the cubic power of the pattern diameter ($8r^3$), pattern collapse becomes an increasingly crucial problem for fine patterns like nanostructures. Equation 1 states that patterns with high aspect ratios and high pattern densities (or narrow distances between the pattern components) are more prone to collapsing when surrounded by high surface-tension liquids. To suppress the capillary cohesive forces caused by the surface tension between the pillars, the surface tension of the liquid must be re-

  

duced, or the contact angle of the liquid must be brought close to 90°. This is done using the well-known concept of supercritical drying with liquid $CO_2$ and reduces the surface tension during solvent drying.[19]

In microcontact printing, the source of stamp-pattern collapse is most likely the capillary force exerted by the ethanol solution on the surface area of the pillars that is beyond the stable/distorted boundary for the given pattern. Once two neighboring pillars make contact, the contact area increases, owing to the action of surface forces near the edge of contact.[20] To reduce the pattern collapse, the aspect ratio and the pattern density should be made lower. A recent 3D simulation of pattern collapse caused by surface tension with changing Young's modulus agrees well with our experimental results.[21]

Next, we investigated the post-stability of two different PDMS materials in replica molding. Figure 4 shows NOA73 replicas of three nanostructures. These results are somewhat surprising and clearly indicate that pattern density plays a more important role than aspect ratio. The patterns ($2r = 0.92$ μm) in Figure 4a have a

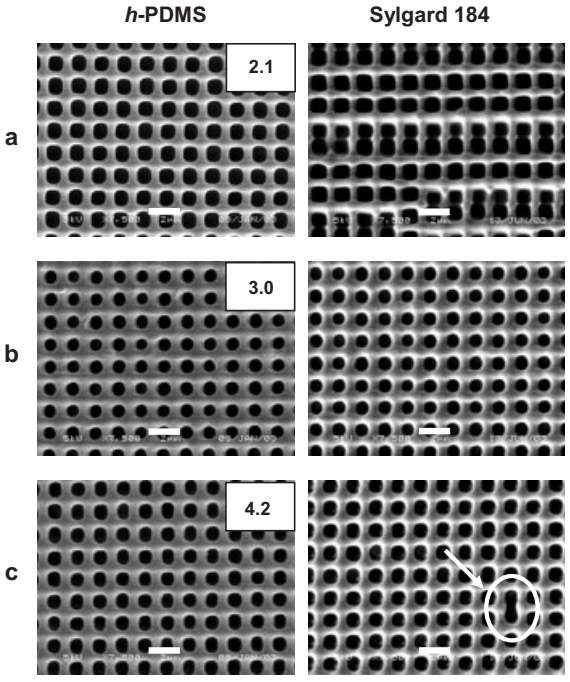


**Figure 4.** SEM images of NOA73 replicas made using two different PDMS stamps (h-PDMS and Sylgard 184). The numbers in the top right corners of the left images indicate the aspect ratios of the posts of the PDMS molds. The same masters used in Figure 3 were used here. In addition, the same masters were used for producing the composite h-PDMS and Sylgard molds. The pattern density of the nanostructure in (a) is 0.303 and that in (b,c) is 0.235. The scale bars are 2 μm. The arrow in (c) indicates collapsed defects that were occasionally observed in high-aspect-ratio replicas prepared with Sylgard 184 molds.

higher pattern density than those ($2r = 0.81$ μm) in Figures 4b,c. The posts of Sylgard 184 PDMS stamps collapse easily when the pattern density is high (0.303), even if the aspect ratio is low (i.e., 2.1), as shown in Figure 4a. On the other hand, the Sylgard 184 PDMS posts with higher aspect ratios but lower pattern densities (0.235) showed fewer defects from lateral collapsing (Figs. 4b,c). Occasionally, we do observe lateral collapse defects in samples with very high aspect ratios (arrow in the right-hand image of Fig. 4c). When composite h-PDMS stamps were used, lateral collapse defects were not found in all cases (left-hand images of Fig. 4). Compared with microcontact printing, replica molding produces fewer defects, although the surface tension of NOA73 (40 mN m$^{-1}$) is higher than that of an ethanolic solution of HDT (22.1 mN m$^{-1}$). This phenomenon results from the fact that, in microcontact printing, the ethanol evaporates from the PDMS stamps after inking and the surface tension pulls on the posts, while in replica molding, the PDMS posts are always surrounded by NOA73 in the case of complete filling.

The molding technique initially includes a capillary force when the NOA73 (i.e., a prepolymer) fills the grooves of the PDMS mold. The filling time, $t$, is defined by Equation 2[22]

$$t = 2\eta H^2/\gamma R\cos\theta \quad (2)$$

where $\eta$ is the prepolymer viscosity, $\gamma$ is the fluid surface tension, $R$ is the hydraulic radius of the capillary, and $\theta$ is the contact angle between the liquid and the surface of the capillary. The viscosity of the NOA 73 prepolymer solution is as low as 130 cP (1 cP = 0.001 Pa s) at 25 °C, which allows rapid filling, as expected from Equation 2. Although the estimated filling time was as short as ≈ 0.5 ms, even for the pattern with an aspect ratio of 6, we allowed the prepolymer solution to fill into the recessed features of the PDMS mold for several minutes. Before complete filling, the PDMS stamp pillars could be deformed by surface tension. However, once the recessed regions of the PDMS stamp are fully filled with the prepolymer solution, the liquid no longer exerted any surface tension. In addition, NOA73 was not allowed to evaporate, unlike the ethanolic solution, for microcontact printing. After complete filling of the prepolymer, the deformed stamp pillars at the initial incomplete filling stage tended to move backwards to the original state, owing to the elasticity of PDMS, as the surface tension was removed upon complete filling. Since NOA73 gets more viscous under UV irradiation, the viscous matter can keep the pillars well separated. This could be the reason why, even though NOA 73 has a higher surface tension, replica molding still generates fewer defects than microcontact printing using a lower-surface-tension ethanolic solution. When the contact area between the merged posts is large, however, adhesive forces can impede the restoration of the pillars. In this case, the prepolymer will be cured as they merge. An example of this is shown in the right-hand image of Figure 4a, which is an image of the replica mold of the low-aspect-ratio (2.1) Sylgard 184 stamp. After the prepolymer was crosslinked by UV irradiation, the elastic modulus of the cured polymer was as high as 1600 psi (11.03 MPa). Therefore, the replicated patterns of NOA73 are not likely to be affected by the removal of the PDMS mold, although there could be a possibility of weak surface tension between the pillars because of the moisture in the air. Figure 4 clearly shows that the stamp deformation during replica molding is not as severe as that during microcontact printing, because of the reasons we described above. For mi-

  

ADVANCED FUNCTIONAL MATERIALS



crocontact printing, in addition to the inking process, stamp-shape changes can also happen during the printing process.[23] As a result, stamp deformation and distortions in the nanopatterns occur more readily in the microcontact printing than in replica molding. All experimental results are summarized in Table 1.

To make the polymerized nanostructures adhere well to the substrate (Fig. 5a), we ensured that the focus position of the laser beam was located at the interface between SU8 and the substrate during the entire scan. However, since we used a piezo tube to scan the sample in the two-photon microscope, if the sample was mounted too far from the center of the scan axis, the focal plane could have deviated from the SU8/substrate interface. Figure 5b shows an example for which three corners became detached from the substrate. Surprisingly, when we performed the replica-molding experiment (Fig. 2g) using this master, the curved structure, which has a true 3D morphology, was replicated in NOA73 (Fig. 5c). This is the result of the flexible mechanical properties of PDMS, and indicates the ability to reproduce complex 3D patterns using soft lithography.

**Table 1.** Summary of pattern fidelity of microcontact-printed patterns (mCP) and NOA replica-mold patterns using two different PDMS stamps (h-PDMS and Sylgard 184).

| Aspect ratio | Pattern density | PDMS | mCP | Molding (NOA73) |
|---|---|---|---|---|
| 2.1 | 0.303 | Sylgard | Collapse (2 posts) | Collapse (2 posts) |
| | | h-PDMS | Good | Good |
| 3.0 | 0.303 | Sylgard | Collapse (4–6 posts) | Collapse (2–4 posts) |
| | | h-PDMS | Collapse (2 posts) | Good |
| 3.0 | 0.235 | Sylgard | Collapse (4–6 posts) | Good |
| | | h-PDMS | Good | Good |
| 3.3 | 0.235 | Sylgard | Collapse (4–8 posts) | Good |
| | | h-PDMS | Collapse (2 posts) | Good |
| 4.2 | 0.235 | Sylgard | Highly collapsed | A few collapsed posts |
| | | h-PDMS | Highly collapsed | Good |

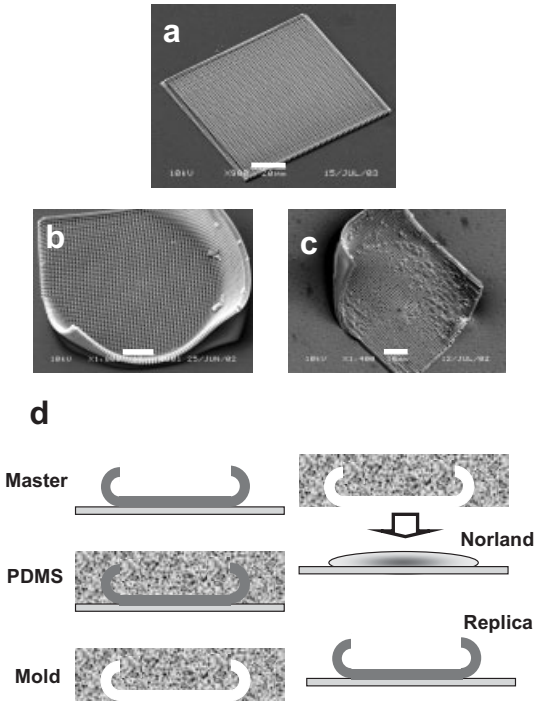


**Figure 5.** The replication of a nanostructure with 3D morphology. The standard (a) and vertically curled (b) nanostructures fabricated by two-photon lithography. The master pattern (b) was replicated to give the replica pattern (c). The top-right of the master pattern (b) corresponds to the top-left of the replica pattern (c). Although the overall 3D morphology was replicated in NOA73, the replica has defects which are the broken posts of the PDMS stamps (bumps in (c)) generated during the molding process. The scale bar in (a) is 20 μm and those in (b,c) are 10 μm. The 3D molding procedure is illustrated in (d).

## 3. Conclusion

We fabricated high-aspect-ratio nanostructures using two-photon laser-scanning lithography to test the deformation and distortion that can arise in soft lithography. We studied the effect of aspect ratio and pattern density of the nanostructures (which can be tuned by varying the laser-scanning parameters, such as the laser-beam power, the laser-scanning rate, and the focal depth) on microcontact printing and replica molding using two commercially available PDMS materials. In agreement with previous work, we found the performance of h-PDMS is superior when dealing with nanostructures. However, we also found that, even when the aspect ratio is low, lateral collapse readily occurs when the pattern density is high. Therefore, pattern density is a more important parameter to consider than aspect ratio when discussing replicating nanostructures in soft lithography. For the two soft-lithography techniques investigated here, microcontact printing and replica molding, we found that good pattern-transfer fidelity is more easily achieved with replica molding. We also showed that replica molding is a promising tool for replicating true 3D morphology as well as nanostructures with aspect ratios of at least ≈ 4.

## 4. Experimental

Our two-photon lithography setup includes a 130 fs, 76 MHz, 710 nm mode-locked Ti:sapphire laser (MIRA900) as the light source and a modified Nikon microscope with a piezo scanner to move the sample with respect to the laser beam, as Figure 1a shows. The polymer material was SU8-5 (Micro Chem Corp.), a negative photoresist commonly used to produce high-aspect-ratio structures. The surface of the glass substrate was treated by oxygen plasma (0.13 torr = 17.33 Pa) for 2 min at 50 W to improve adhesion between the polymerized SU8 and the glass. After spinning the SU8 films on the substrate, the film was prebaked at 65 °C for 30 min. The laser beam was focused with a Nikon 100× objective (0.95 numerical aperture, NA) at the interface of the glass and SU8, to make photopolymerized structures attach to the glass substrate. The sample was scanned at a speed between 25 and 110 $\mu m\,s^{-1}$ and the average laser power was varied between 3 and 9 mW. The maximum peak intensity at the focus ranged from 107 to 322 $GW\,cm^{-2}$. To complete photopolymerization, the SU8 film was post-baked at 65 °C for 20 min and then at 90 °C for 90 s. To avoid collapse of the high-aspect-ratio structures, the post-baked pattern underwent supercritical $CO_2$ drying after developing.

The molds were made using Sylgard 184 (Dow Corning, Midland, MI) and h-PDMS. The Sylgard 184 was mixed in a 10:1 ratio of prepolymer and curing agent. Before casing the mixture, it was degassed

  

in a vacuum. After heating the cast mixture on the master at 60 °C for 2–3 h, we peeled off the mold from the master. The composite h-PDMS stamps were composed of two layers (a thin, stiff h-PDMS layer supported by a thick, flexible Sylgard 184 layer). To prepare h-PDMS, we mixed a vinyl PDMS prepolymer (3.4 g; VDT-731, Gelest Inc., Morrisville, PA), a platinum catalyst (one drop; platinum divinyltetramethyldisiloxane, SIP6831.1, Gelest Inc.), and a modulator (one drop; 2,4,6,8-tetramethyl- tetravinylcyclotetrasiloxane, 87927, Sigma-Aldrich). After degassing for about 15 min, hydrosilane prepolymer (1 g; HMS-301, Gelest Inc.) was gently stirred into this mixture. It was then degassed for another ≈2 min. We then spin-coated a ≈40 μm layer of h-PDMS onto the master (800 rpm, 85 s) and cured it for 10–15 min in a 60 °C oven. A liquid prepolymer layer (≈3–4 mm) of Sylgard 184 PDMS was poured onto the h-PDMS layer and cured for 2–3 h at 60 °C. After taking the composite mold out of the oven, we immediately peeled the stamp carefully off the master.

The first step of microcontact printing was inking PDMS stamps with a ≈2 mM ethanolic solution of hexadecanethiol and bringing the stamps into contact with the gold-coated (Au(15 nm)/Ti(1 nm)) silicon wafer for ≈5 s. The resulting SAM patterns are in the same geometry as the stamp and act as a protective layer for subsequent gold etching. Soaking in an aqueous ferricyanide etchant for 8 min removed the gold that was not protected by the printed SAM, and produced gold patterns [24]. For replica molding, we put a drop of an optical adhesive, NOA73 (Norland Product Inc., NJ), on a flat surface (e.g., glass slides) and brought the PDMS molds into contact on top of the optical adhesive (Fig. 2g) before illuminating it with a UV lamp (wavelength of 365 nm) for 5 h.

Received: July 2, 2004
Final version: May 31, 2005
Published online: September 1, 2005

[1] Y. Xia, G. M. Whitesides, *Angew. Chem. Int. Ed.* **1998**, *37*, 550.
[2] Y. Xia, J. A. Rogers, K. E. Paul, G. M. Whitesides, *Chem. Rev.* **1999**, *99*, 1823.
[3] J. Aizenberg, A. J. Black, G. M. Whitesides, *Nature* **1999**, *398*, 495.
[4] X.-M. Zhao, S. P. Smith, S. J. Waldman, G. M. Whitesides, M. Prentiss, *Appl. Phys. Lett.* **1997**, *71*, 1017.
[5] M. V. Kunnavakkam, F. M. Houlihan, J. A. Liddle, P. Kolodner, O. Nalamasu, J. A. Rogers, *Appl. Phys. Lett.* **2003**, *82*, 1152.
[6] T. W. Odom, J. C. Love, D. B. Wolfe, K. E. Paul, G. M. Whitesides, *Langmuir* **2002**, *18*, 5314.
[7] H. Schmid, B. Michel, *Macromolecules* **2000**, *33*, 3042.
[8] Ch. J. Schwartz, A. V. V. Nampoothiri, J. C. Jasapara, W. Rudolph, S. R. J. Brueck, *J. Vac. Sci. Technol. B.* **2001**, *19*, 2362.
[9] S. Kawata, H.-B. Sun, T. Tanaka, K. Takada, *Nature* **2001**, *412*, 697.
[10] S. Maruo, O. Nakamura, S. Kawata, *Opt. Lett.* **1997**, *22*, 132.
[11] B. H. Cumpston, S. P. Ananthavel, S. Barlow, D. L. Dyer, J. E. Ehrlich, L. L. Erskine, A. A. Heikal, S. M. Kuebler, I. Y. S. Lee, D. McCord-Maughon, J. Qin, H. Rockel, M. Rumi, X.-L. Wu, S. R. Marder, J. W. Perry, *Nature* **1999**, *398*, 51.
[12] H.-B. Sun, S. Matsuo, H. Misawa, *Appl. Phys. Lett.* **1999**, *74*, 786.
[13] T.-W. Lee, O. Mitrofanov, C. A. White, J. W. P. Hsu, *Mater. Res. Soc. Symp. Proc.* **2003**, *776*, Q8.32.1.
[14] J. Squier, M. Muller, *Rev. Sci. Instrum.* **2001**, *72*, 2855.
[15] H.-B. Sun, T. Tanaka, S. Kawata, *Appl. Phys. Lett.* **2002**, *80*, 3673.
[16] S. Juodkazis, V. Mizeikis, K. K. Seet, M. Miwa, H. Misawa, *Nanotechnology* **2005**, *16*, 846.
[17] H. Namatsu, K. Kurihara, M. Nagase, K. Iwadate, K. Murase, *Appl. Phy. Lett.* **1995**, *66*, 2655.
[18] T. Tanaka, M. Morigami, N. Atoda, *Jpn. J. Appl. Phys., Part 1* **1993**, *32*, 6059.
[19] D. L. Goldfarb, J. J. de Pablo, P. F. Nealey, J. Simons, W. M. Moreau, M. Angelopoulos, *J. Vac. Sci. Technol. B* **2000**, *18*, 3313.
[20] E. Delamarche, H. Schmid, B. Michel, H. Biebuyck, *Adv. Mater.* **1997**, *9*, 741.
[21] M. Kotera, N. Ochiai, *Microelectron. Eng.* **2005**, *78–79*, 515.
[22] D. Myers, *Surfaces, Interfaces and Colloidals*, Wiley-VCH, New York **1999**.
[23] C. Y. Hui, A. Jagota, Y. Y. Lin, E. J. Kramer, *Langmuir* **2002**, *18*, 1394.
[24] A. Kumar, G. M. Whitesides, *Appl. Phys. Lett.* **1993**, *63*, 2002.

  